Eur Biophys J (1986) 13:203–218

European Biophysics Journal

The human erythrocyte membrane skeleton may be an ionic gel

I. Membrane mechanochemical properties

B. T. Stokke*, A. Mikkelsen, and A. Elgsaeter

Division of Biophysics, University of Trondheim, N-7034 Trondheim – NTH, Norway

Received June 17, 1985/Accepted October 15, 1985

Abstract. Biochemical and biophysical observations indicate that the erythrocyte membrane skeleton is composed of a swollen network of long, flexible and ionizable macromolecules located at the cytoplasmic surface of the fluid membrane lipid bilayer. We have analyzed the mechanochemical properties of the erythrocyte membrane assuming that the membrane skeleton constitutes an ionic gel (swollen ionic elastomer). Using recently established statistical thermodynamic theory for such gels, our analysis yields mathematical expressions for the mechanochemical properties of erythrocyte membranes that incorporate membrane molecular parameters to an extent not achieved previously. The erythrocyte membrane elastic shear modulus and maximum elastic extension ratio predicted by our membrane model are in quantitative agreement with reported values for these parameters. The gel theory predicts further that the membrane skeleton modulus of area compression, K_G, may be small as well as large relative to the membrane elastic shear modulus, G, depending on the environmental conditions. Our analysis shows that the ratio between these two parameters affects both the geometry and the stability of the favoured cell shapes.

Key words: Erythrocyte, spectrin, protein gel, membrane skeleton, membrane model

Introduction

The highly symmetric biconcave shape of the human erythrocyte has led to continued interest in the molecular mechanisms giving rise to this characteristic and usual shape. Numerous studies suggest that spectrin is involved in determining the mechanical properties and stable shapes of human erythrocytes by forming a macromolecular network at the cytoplasmic surface of the lipid bilayer (Branton et al. 1981; Bennett 1982; Cohen 1983; Goodman and Shiffer 1983; Gratzer 1983; Gratzer 1984). The mechanical behaviour of the erythrocyte membrane (Evans 1973; Waugh and Evans 1979; Evans and Skalak 1979) and the salt, pH and temperature dependent shape changes both in human erythrocytes and delipidated erythrocyte ghosts (Johnson and Robinson 1976; Johnson et al. 1980) are all manifestations of the erythrocyte membrane composition, organization and interactions both within the membrane and between the membrane and the environment. Currently, the two main hypotheses put forward to account for the biconcave shape are the uniform shell hypothesis (Canham 1970) and the bilayer couple hypothesis (Sheetz and Singer 1974). The former has subsequently been extended to incorporate both membrane shear resistance and bending resistance (Deuling and Helfrich 1976; Evans and Skalak 1979). The shear resistance in the uniform shell hypothesis was attributed to the membrane skeleton (Evans 1973). The bilayer couple hypothesis is based on an assumed preferential perturbation of either the extra- or the intra-cellular half of the membrane lipid bilayer by various shape change inducing agents (Sheetz and Singer 1974).

Based on currently available information on the physical properties of spectrin and the molecular organization of the erythrocyte membrane we advance the hypothesis that the erythrocyte membrane skeleton constitutes an ionic gel (swollen ionic elastomer) in close proximity to the lipid bilayer. It has recently been discovered that ionic gels exhibit critical phenomena and phase transitions (Tanaka et al. 1980) and that these and other mechanochemical properties of such ionic gels can be analyzed using standard methods of statistical thermodynamics (Flory 1953; Treloar 1975; Flory 1976, 1977; Tanaka et al. 1980). Using this new information we

* To whom offprint requests should be sent

here develop and discuss mechanochemical properties, elastic free energy, cell shapes, and cell shape stability of human erythrocytes in terms of a new protein gel – lipid bilayer membrane model where the membrane skeleton is assumed to constitute an ionic gel.

Although our continuum mechanical analysis of the erythrocyte membrane uses many of the same concepts and leads to many of the same considerations that have been used by others (Canham 1970; Evans and Skalak 1979) our model for the first time introduces the properties of ionic gels into the analysis of red cell shape. By considering the membrane skeleton to be an ionic gel, the membrane skeleton mechanochemical properties are given a coherent molecular and theoretical basis that is firmly grounded on recent biochemical and ultrastructural observations. From a purely continuum mechanical point of view the main difference between the new concept and previous models is that the modulus of area compression of the membrane skeleton may be large as well as small relative to the membrane skeleton elastic shear modulus and that, because of this, the membrane skeleton area density may be non-uniform. The erythrocyte membrane elastic shear modulus and maximum elastic extension ratio predicted by the protein gel – lipid bilayer membrane model are in quantitative agreement with reported values for these parameters. Numerical analyses of erythrocyte shapes, shape stability and shape transformations by Stokke et al. (1986) show that the new concept can account for all the commonly observed erythrocyte shapes and shape transformations.

The spectrin network

The two polypeptides (α and β) that make up the spectrin dimer have molecular weights of about 240,000 and 220,000 Daltons (Steck 1974). Electron microscopic studies of spectrin heterodimers have revealed that these molecules consist of two 100 nm long, flexible subunits interconnected at both ends (Shotton et al. 1979). Spectrin heterodimers can associate head-to-head to form 200 nm long spectrin heterotetramers (Shotton et al. 1979). Both in vivo and in vitro there is a slow association equilibrium between spectrin heterodimers and heterotetramers (Ungewickell and Gratzer 1978; Liu and Palek 1980). Light scattering, birefringence relaxation, viscometric and electron paramagnetic resonance (EPR) studies of isolated spectrin confirm that the spectrin molecules are long and flexible (Ralston 1976; Elgsaeter 1978; Mikkelsen and Elgsaeter 1978, 1981; Lemaigre-Dubreuil et al. 1980; Stokke and Elgsaeter 1981; Dunbar and Ralston 1981; Reich et al. 1982; Lemaigre-Dubreuil and Cassoly 1983) with a persistence length of about 20 nm (Mikkelsen et al. 1984; Stokke et al. 1985a). This is consistent with the reported amino acid sequence of the spectrin molecule which indicates that each α- and β-chain consists of 20 and 18 rather stiff, almost identical, regions connected by quite flexible joints (Speicher and Marchesi 1984). The temperature dependence of the intrinsic viscosity of isolated spectrin dimers indicates further that the lowest internal energy of the spectrin dimers is associated with the fully extended conformation and that spectrin dimers in solution are therefore essentially "entropy springs" (Stokke et al. 1985a).

It is well established that the spectrin molecules in vivo form a meshwork on the cytoplasmic side of the erythrocyte membrane lipid bilayer (Nicolson et al. 1971; Steck 1974). Tyler et al. (1980) and Liu and Palek (1980) obtained evidence suggesting that spectrin heterotetramers constitute the chains of this spectrin network. Cohen et al. (1980) found that actin oligomers may be an integral part of the network junctions and that the maximum junction functionality may be determined by the length of the actin oligomers. The length of these oligomers may be controlled by protein 4.9 which has been reported to be an actin bundling protein (Siegel and Branton 1985). This led to the notion that each gel chain consists of one spectrin tetramer (Cohen 1983). Byers and Branton (1985) have succeeded recently in direct electron microscopic visualization of the proteins associated with the erythrocyte membrane skeleton and their findings confirm many of these earlier conclusions. However, because of the association equilibrium between the α and β spectrin subunits it is also possible that the two α and two β subunits of one such gel chain are part of three or even four separate spectrin dimers (Fig. 1) (Tyler et al. 1980; Morrow and Marchesi 1981). This does change the apparent topology of the intact network, but disruption of the network by weakening the spectrin-actin binding under conditions that trap the $\alpha-\beta$ subunit association will in the first case give tetramers only, whereas the latter case also yields higher order spectrin oligomers (Fig. 1). Such higher order spectrin oligomers are observed frequently in low ionic strength, low temperature extracts of erythrocyte membranes (Liu et al. 1984).

The number of spectrin dimers per erythrocyte is about 240,000 (Steck 1974). If we assume that the spectrin dimer has a length of 100 nm and a circular cross section with the same diameter along the entire length of the molecule, that the dimer molecular weight is 460,000 daltons, that the spectrin density is 1.37 g/cm^3 (Kam et al. 1977), and that the

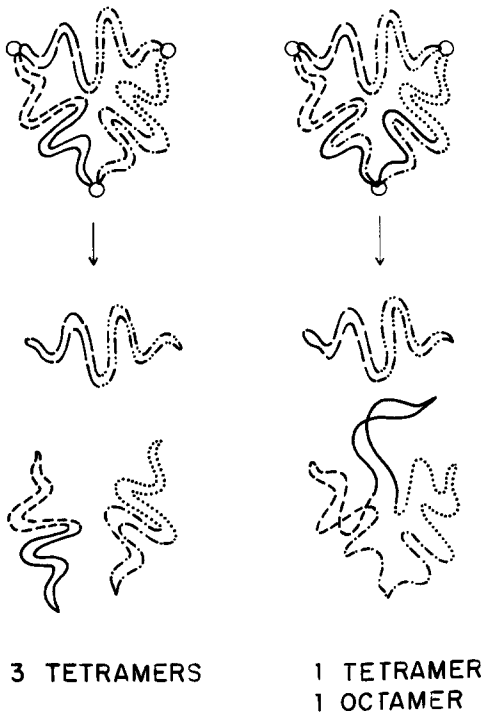

Fig. 1. Schematic illustration of spectrin oligomer formation in a spectrin network where there is an association equilibrium between the spectrin α and β subunits. The diagram shows three junction points (*circles*) representing the multivalent actin, band 4.1, band 4.9 complexes that cross-link the spectrin tetramers (*solid, dotted* and *dashed lines*). On the left it is assumed that the individual α and β subunits in each heterodimer are associated with the α and β of only one other heterodimer. Dissociation of the network by eliminating the cross-linking junction points produces only tetramers. On the right it is assumed that the individual α and β subunits in one of the heterodimer associate with the α and β subunits of two separate heterodimers. Dissociation of this network can then yield higher order oligomers, such as the octamer shown

spectrin is packed as a monolayer, then all the spectrin in one cell would cover an area of approximately 64 μm^2. This is about 45% of the total cell surface area of about 140 μm^2 (Canham 1970). The spectrin molecules are ionizable with isoelectric point about pH 4.8 (Elgsaeter et al. 1976). Unless the intramolecular thermal motion of the spectrin molecules is suppressed when they are part of the membrane skeleton, this structural information leads to the conclusion that the erythrocyte membrane skeleton most likely constitutes an ionic gel. EPR measurements of spectrin in solution and spectrin bound to the membrane show no evidence of immobilization of the spectrin molecules as a result of the binding of spectrin to the membrane (Lemaigre-Dubreuil et al. 1980; Lemaigre-Dubreuil and Cassoly 1983). Recently, measurements of the elastic properties of 3-dimensional macroscopic spectrin networks have been reported (Schanus et al. 1985; Stokke et al. 1985b). Although the reconstitution approach used in these studies are different, both reports indicate that the elastic component of the viscoelasticity of these spectrin containing networks may be accounted for by simple elastomer theory.

The protein gel – lipid bilayer membrane model

The currently available biochemical and biophysical evidence on the physical properties of spectrin in solution and the molecular organization of the erythrocyte membrane skeleton described above is summarized in what we have chosen to refer to as the protein gel – lipid bilayer membrane model. We assume that the membrane consists of a fluid lipid bilayer and an apposed protein membrane skeleton that constitutes an ionic gel (swollen ionic elastomer) (Figs. 2 and 3). The gel network is assumed to depend in part on non-covalent bonds. The time average equilibrium gel topology of the spectrin network may depend on the environmental conditions, but the time constant involved in such changes (Ungewickell and Gratzer 1978) appears to be long relative to the characteristic times of commonly observed cell shape changes (Lange et al. 1982). We assume that the two halves of the lipid bilayer and the ionic protein gel all are free to slide relative to one another in the plane of the cell membrane. We

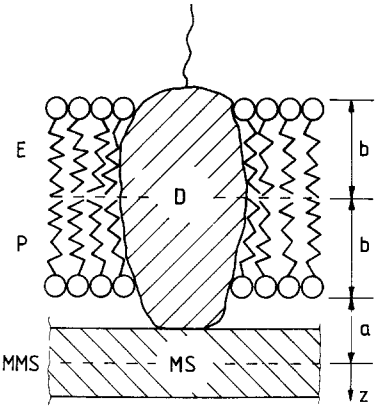

Fig. 2. Schematic illustration of the protein gel – lipid bilayer cell membrane model. The lipid molecules of the extracellular (*E*) and protoplasmic (*P*) half of the membrane lipid bilayer are in the fluid state. Each half of the lipid bilayer has thickness *b*. The membrane skeleton (*MS*) behaves like an ionic gel (swollen ionic elastomer). The distance from the middle of the membrane skeleton (*MMS*) to the lipid bilayer cytoplasmic surface is *a*. Coordinate *z* is the distance from MMS and is positive for points located on the cytoplasmic side of MMS and negative if the point is located at the opposite side of MMS. Integral membrane proteins (*D*) may or may not be linked to the membrane skeleton. The two halves of the membrane lipid bilayer and the membrane skeleton are all free to slide relative to one another in the plane of the cell membrane. The membrane skeleton may change its density distribution as the cell shape is changed

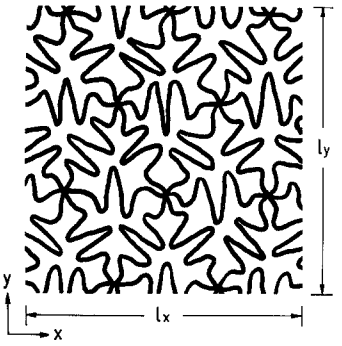

Fig. 3. Schematic illustration of a two-dimensional gel with repeating topological patterns where the junction functionality $\Phi = 6$ and the spatial and topological first neighbour junctions are the same. The unit of a gel that extend between two topological first neighbour junctions we refer to as a chain of the gel. A single chain of a protein gel may correspond to one polypeptide, to only a fraction of a polypeptide, or to several polypeptides. The area fraction covered by the gel chains, $\varphi' = A_M/(l_x l_y)$, where A_M is the surface area of the macromolecules making up the gel, is always less than one

find that, depending on the environmental conditions, the gel modulus of area compression, K_G, may be large as well as small relative to the elastic shear modulus, G. When the environmental conditions are such that the gel modulus of area compression is much larger than the gel elastic shear modulus, the membrane skeleton will behave as an incompressible two-dimensional solid as discussed by Skalak et al. (1973), Evans (1973), Brailsford et al. (1976), Evans and Skalak (1979), Evans and Buxbaum (1981) and others. However, under other environmental conditions, where K_G is of the same order of magnitude or smaller than G one has to take into account the possible effects of a compressible gel. We find that for this situation the gel density distribution in the plane of the membrane for a given cell shape generally no longer will be uniform.

The spectrin gel elastic shear modulus

A two-dimensional macromolecular gel is defined as a swollen two-dimensional cross-linked network of long, flexible macromolecules undergoing thermal motions. The gel area fraction, φ', is defined as the area accounted for by the macromolecules relative to the total area spanned by the macromolecules. For a gel, φ' is always less than one (Fig. 3). The functionality of a junction, Φ, equals the number of chains extending from a junction.

When there is no gel chain intra- or intermolecular interactions and when the chains are unionized, the elastic free energy of the gel is of purely entropic origin and is referred to the "rubber elasticity" of the gel. The change in elastic free energy of a two-dimensional gel area element which in the reference state is square-shaped with sides l_r and in the deformed state rectangular with sides l_x, l_y (Flory 1976):

$$\Delta F_i = \tfrac{1}{2} N_c\, k\, T\, ((l_x/l_r)^2 + (l_y/l_r)^2 - 2) - (2/\Phi)\, N_c\, k\, T \ln (l_x l_y / l_r^2)\,, \quad (1)$$

where N_c is the number of chains in the two-dimensional gel area element under consideration, k is the Boltzmann constant, and T is the absolute temperature. The gel is assumed to have negligible boundary effects, junctions subjected to affine displacement, suppressed junction fluctuations, and gel chains following Gaussian statistics. In the reference state the chain configuration is the same as for free chains. If junctions of different functionality are present, but with $\Phi \geq 3$ for all of them, then Φ is the average functionality. Equation (1) is valid independent of the orientation of the x- and y-axes relative to the details of the gel topology.

For a gel area element which in the reference state is a square with sides l_r the elastic shear modulus G measured in a state where the gel area element has surface area l_u^2, equals (Treloar 1975; Flory 1976):

$$G = k\, T\, (N_c/l_u^2)\, \langle l_u^2 \rangle / \langle l_r^2 \rangle\,. \quad (2)$$

Note that Eq. (2) is valid for the gel topology illustrated in Fig. 3 as well as for randomly cross-linked two-dimensional gels. It is also important to note that Eq. (2) does not require that the gel chains are truly random coil chains. The only requirement is that the end-to-end distance has a Gaussian distribution (Flory 1976) which is found to be true for most flexible and highly elongated macromolecules (Cantor and Schimmel 1980).

Assuming that one spectrin heterotetramer constitutes one gel chain and using the number of spectrin heterotetramers per erythrocyte and the erythrocyte surface area referred to above, yields $N_c/l_u^2 \approx 780\ \mu m^{-2}$. The ratio $\langle l_u^2 \rangle / \langle l_r^2 \rangle$ is unknown, but because of the slow kinetics of the association equilibrium between the components of the spectrin network this ratio may be expected to be close to one. This yields $G \approx 3 \times 10^{-3}$ dyne/cm at room temperature for the human erythrocyte spectrin network. If each of the two subchains of the heterotetramers undergoes independent thermal motions, the predicted value of G equals 6×10^{-3} dyne/cm. The presence of higher order spectrin oligomers as depicted in Fig. 1 does not alter this theoretically predicted value. Since the membrane lipid bilayer is assumed to be in the fluid state this also equals the predicted value of the elastic shear modulus for the whole erythrocyte membrane.

Several authors have measured the pressure required to aspirate a certain fraction of an erythrocyte into a microcapillary, and have from these data calculated the membrane elastic shear modulus. Waugh and Evans (1979) reported $G = (6.6 \pm 1.2) \times 10^{-3}$ dyne/cm at 25 °C and Chien et al. (1978) reported $G = 4.3 \times 10^{-3}$ dyne/cm. The agreement between the value of G predicted by the protein gel – lipid bilayer membrane model and these experimental values is remarkable. Our experimental data indicate that isolated spectrin free in solution or cross-linked in vitro into macroscopic three-dimensional networks behave essentially like entropy springs (Stokke et al. 1985a, b). However, because of the possible interactions between the spectrin in the membrane skeleton and the lipid bilayer it is not at all obvious that the spectrin molecules would behave as entropy springs also when they are part of the membrane skeleton. The agreement between the experimental value of G and the value of G predicted theoretically from gel theory strongly suggests that spectrin molecules in situ also behave essentially like entropy springs and that the membrane skeleton therefore does constitute an ionic gel. Equation (2) yields

$$(T/G)\,\partial G/\partial T = 1 + T\partial \ln N_c/\partial T - T\partial \ln \langle l_r^2 \rangle/\partial T. \quad (3)$$

The temperature dependence of the end-to-end distance of spectrin dimers estimated from intrinsic viscosity (Stokke et al. 1985a) indicates that $T\partial \ln \langle l_r^2 \rangle/\partial T = -(1.2 \pm 0.6)$. Waugh and Evans (1979) found that the membrane elastic shear modulus decreased with increasing temperature. Their experimental data yield $(T/G)\,\partial G/\partial T = -(3 \pm 1)$ in the temperature range 5–35 °C. If the membrane skeleton behaves like a swollen elastomer this implies that the number of effective network strands, N_c, has to decrease with increasing temperature. An estimate of $T\partial \ln N_c/\partial T$ can be obtained by assuming that the spectrin network consists of tetramers in equilibrium with dimers and each tetramer constitutes two gel chains. It can then be shown that

$$T\partial \ln N_c/\partial T = T\partial \ln K_A/\partial T/\sqrt{(1 + 16 K_A[S])}\,, \quad (4)$$

where K_A is the spectrin dimer-tetramer association constant and $[S]$ is the tetramer concentration when all the spectrin is present as tetramers. The numerical values of K_A in the absence of other molecules, in the temperature range 25–37 °C, obtained by Ungewickell and Gratzer (1978) yield a value of $T\partial \ln N_c/\partial T$ ranging from -1 to -3 when the effective gel thickness is assumed to be 20 nm. However, it should be noted that Liu and Palek (1984) reported that hemoglobin enhances the self-association of spectrin dimers. The network junction integrity may also be temperature dependent. Enough experimental data on the thermoelastic properties of the spectrin network to make a quantitative comparison between the experimental data of Waugh and Evans (1979) and the behaviour predicted by our membrane model is therefore not yet available, but the observed temperature dependence of the erythrocyte elastic shear modulus is clearly not incompatible with modern gel theory.

The spectrin gel maximum elastic extension ratio

The extension ratio of a square gel element with edge lengths l_r which is deformed to length l_x in the x-direction equals $\varepsilon \equiv l_x/l_r$. For gels with gel chains consisting of a finite number, N_s, of freely jointed segments, the Gaussian chain statistics is not valid when l_x approaches the chain contour length and ε can only be increased up to a certain value, ε_{max}, without rupture of some of the gel linkages.

The effect of finite ε_{max} is clearly illustrated by calculating the force, f_x, needed in the x-direction to maintain the isotropic deformation l_r, $l_r \to l_x$, $l_y = l_x$ (Treloar 1975) using non-Gaussian chain statistics:

$$f_x = (N_c/3)\,(kT/l_r)\sqrt{N_s}\,L^{-1}(l_x/(l_r\sqrt{N_s})) - (2N_c/\Phi)\,(kT/l_r)\,(l_r/l_x)\,, \quad (5)$$

where

$$L(\beta) = \coth(\beta) - 1/\beta = \text{Langevin function} \quad (6)$$

and L^{-1} is the inverse Langevin function. When $N_s \to \infty$ the chains follow Gaussian statistics. Figure 4 shows f_x versus ε for some selected values of N_s. For non-Gaussian chains the maximum extension ratio $\varepsilon_{max} \approx N_s l_s/\langle l_{e-e} \rangle$ where l_s is the length of each identical segment making up a gel chain, $\langle l_{e-e} \rangle$ is the time average end-to-end distance of the gel chains in the reference state and thus the time average distance between topological first neighbour junctions. The contour length, l_c, of a gel chain equals $N_s l_s$. Since $\langle l_{e-e} \rangle \approx l_s\sqrt{N_s}$ this yields $\varepsilon_{max} \approx \sqrt{N_s}$.

For chains which strictly follow Gaussian chain statistics, N_s and thus ε_{max} is infinite (Fig. 4). For a gel not in its reference state $\varepsilon_{max} \approx l_c/\langle l_{n-n} \rangle$ where $\langle l_{n-n} \rangle$ is the time average distance between nearest neighbour junctions. The calculated values of $\langle l_{n-n} \rangle$, ε_{max}, and N_s for the erythrocyte membrane skeleton, assuming that spectrin heterotetramers constitute the gel chains, are shown in Table 1. If the topological first neighbour junctions of the spectrin network are not assumed to be the nearest neighbour junctions, the expected value of ε_{max} would be smaller than the values given in Table 1 by at least a factor of two.

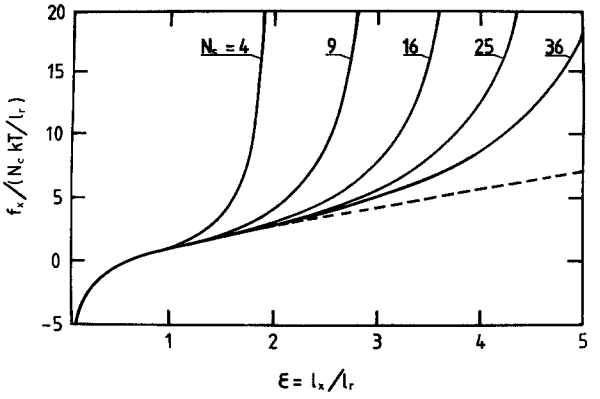

Fig. 4. The force due to the "rubber elasticity" for isotropic expansion/compression of a two-dimensional gel versus extension ratio ε. Gaussian chain statistics (------) (derived from Eq. (1)) and non-Gaussian chain statistics (——) (Eq. (5)) for various numbers, N_s, of freely jointed identical segments per chain. Gel junction functionality $\Phi = 4$. Note that the maximum extension ratio equals $\sqrt{N_s} = l_c/\langle l_{n-n}\rangle$ and that for Gaussian chain statistics $N_s = \infty$

Table 1. Calculated time average distance, $\langle l_{n-n}\rangle$, between nearest neighbour spectrin tetramer network junctions assuming that the spectrin network is topologically replicating, contains 120,000 chains each of length $l_c = 200$ nm and that the total network surface area equals 140 μm². All junctions are assumed to have functionality Φ. ε_{max} is maximum macroscopic extension ratio of the network, calculated using $\varepsilon_{max} \approx l_c/\langle l_{n-n}\rangle$. Parameter N_s is the approximate equivalent number of identical freely jointed segments per chain assuming that the time average gel chain configuration of the nondeformed network is the same as for the free chains. N_s is calculated using $\varepsilon_{max} \approx \sqrt{N_s}$.

Φ	$\langle l_{n-n}\rangle$/nm	ε_{max}	N_s
3	41	~ 5	~ 25
4	52	~ 4	~ 16
6	70	~ 3	~ 9

Evans and LaCelle (1975) found experimentally that the maximum elastic extension ratio of erythrocyte membranes is 3–4. The calculated parameter values given in Table 1 shows that the reported experimental value of ε_{max} is compatible with a replicating network of spectrin tetramers where the topological first neighbour junctions are also the nearest neighbour junctions and have an average junction functionality of 4–6. This is also the functionality observed most often by Byers and Branton (1985). The observed value of ε_{max} further suggests that N_s equals 10–15. This implies that for extension ratios less than 1.5–2.0, the mechanical properties of a spectrin gel may be well accounted for using Gaussian chain statistics (Fig. 4).

The spectrin gel modulus of area compression

The tension needed to expand or compress isotropically an ionic gel depends not only on the entropy of the macromolecules constituting the network, but also on the gel chain intra- and intermolecular interactions and the degree of ionization of the gel chains. As a first approximation, the osmotic surface tension, Π_G, of an ionic two-dimensional protein gel with negligible boundary effects is analogous to the expression for the osmotic pressure of three-dimensional gels (Flory 1953; Treloar 1975; Tanaka et al. 1980):

$$\Pi_G = -(N_A kT/V_1)(\varphi' + \ln(1-\varphi') + (\Delta F_c/2kT)\varphi'^2) - \partial(\Delta F_r)/\partial l_r^2 + \nu_r kTg\varphi'/\varphi_r', \quad (7)$$

where N_A is the Avogadro number, V_1 is the equivalent molar area of the gel solvent, ΔF_c is the chain-chain affinity (a measure of the free energy decrease associated with the formation of contact between chain segments), g is the number of effective dissociated hydrogen ions per chain, and ν_r is the number of chains per unit area in the gel reference state. φ_r' is the area fraction covered by the gel chains in the reference state and

$$\varphi_r'/\varphi' = l^2/l_r^2. \quad (8)$$

The modulus of area compression of the two-dimensional gel is:

$$K_G(l^2) = -l^2\partial\Pi_G/\partial l^2. \quad (9)$$

Equations (7) and (9) predict that K_G may be negative for certain combinations of the molecular parameters, but thermodynamic analysis shows that K_G must be greater than or equal to zero to correspond to a stable equilibrium (ter Haar and Wergeland 1966). Phase transitions and critical phenomena are therefore inherent properties of ionic gels (Tanaka et al. 1980).

To get a rough estimate of the values of Π_G predicted by the protein gel lipid bilayer membrane model, Fig. 5 shows Π_G versus $\langle l_u^2\rangle/\langle l_r^2\rangle$ using several values of the chain-chain affinity and values of other molecular parameters which may be reasonable for the erythrocyte membrane skeleton. Non-Gaussian chain statistics (Treloar 1975) were used to incorporate finite extensibility of the gel chains. The horizontal regions of Π_G were obtained using Eqs. (1) and (7) and Maxwell's rule (ter Haar and Wergeland 1966). For these horizontal regions of Π_G the two-dimensional gel is separated into one dense phase present as patches distributed approximately uniformly within a less dense phase, or vice versa. It is important to note that such phase separation cannot take place without concominant shear

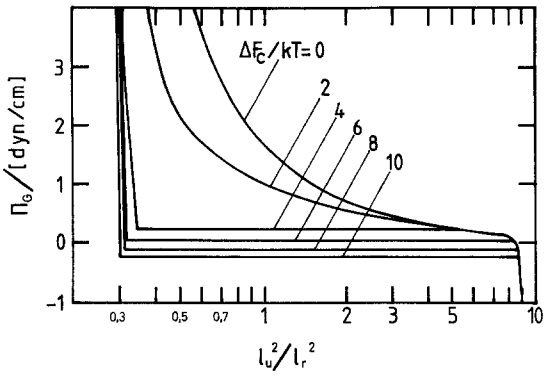

Fig. 5. The osmotic surface tension, Π_G, of an ionic two-dimensional macromolecular gel versus l_u^2/l_r^2, calculated using Eq. (7) and Maxwell's rule. The molecular parameters were chosen to correspond roughly to those of the human erythrocyte spectrin network: $\varphi_i' = 0.3$, $\nu_r' = 1{,}600\ \mu m^{-2}$, $N_s = 9$, $g = 200$, $\Phi = 4$ and $V_1 = 0.5\ nm^2$. The osmotic surface tension is shown for several values of $\Delta F_c/kT$. The actual value of ΔF_c for a spectrin network is not known

deformation due to the topological restraints of the gel. This means that when such gel phases coexist there will be boundary effects and the gel free energy will depend on the geometry of the phase boundaries between the two phases. For this situation, K_G will therefore be small, but not exactly zero. Because the erythrocyte intramembrane particles are partly bound to and partly trapped within the membrane skeleton (for review see Branton et al. 1981) such phase separation will be expected to lead to reversible freeze-etch particle aggregation. The existence of reversible freeze-etch particle aggregation in erythrocyte membranes is well established (Pinto da Silva 1973; Elgsaeter and Branton 1974).

Because K_G is the derivative of Π_G, Fig. 5 indicates that for some environmental conditions K_G of the erythrocyte membrane skeleton is small and probably of approximately the same order of magnitude as G, whereas for other environmental conditions K_G is 2 to 4 orders of magnitude larger than G. These large values of K_G are approximately of the same order of magnitude as the modulus of area compression reported for the whole erythrocyte membrane under one set of environmental conditions studied by Waugh and Evans (1979). It is currently not known how much the human erythrocyte membrane skeleton contributes to the modulus of area compression of the whole erythrocyte membrane.

Cell shape dependent changes in the free energy of the two-dimensional membrane ionic gel

We assume that there exists a reference shape (neutral shape), Ψ_r, for which the time average gel chain configuration is the same as for the free chains, the gel density is uniform, and there is no gel shear deformation. Because of the surface area limitations imposed by the membrane lipid bilayer, it is also useful to define another reference shape, Ψ_u, obtained by linear scaling of Ψ_r. Also for the latter cell shape the gel density is uniform and there is no gel shear deformation, but the gel chains no longer have the same time average configurations as the free gel chains. We will later describe how this reference shape is chosen.

When the cell shape, and hence the membrane skeleton shape, is changed from Ψ_u to some arbitrarily deformed cell shape, Ψ_d, this generally results in deformation of the gel. At the molecular level, the spectrin network obviously does not constitute a continuum. However, limiting ourselves to situations where the time average gel density does not vary significantly within the time average distance between gel nearest neighbour junctions, $\langle l_{n-n} \rangle$, one can still use the standard methods of classical continuum mechanics including the formalism of infinitesimal area elements to analyse the gel free energy. An infinitesimal square gel area element with edge lengths l_u for skeletal shape Ψ_u and with edges oriented parallel to the local principal axes of deformation, will generally be deformed into a rectangle with lengths l_x and l_y on Ψ_d. It is convenient to consider this deformation as consisting of two steps: the first being a pure isotropic expansion $l_u, l_u \to l_l, l_l$ and the second a pure shear deformation at constant gel surface area $l_l, l_l \to l_x, l_y$. During an isotropic area change, the change in the gel elastic free energy per unit gel area of Ψ_u is given by:

$$\Delta F_l = -\int_{l_u^2}^{l_l^2} \Pi_G(l^2)\, dl^2/l_u^2 . \tag{10}$$

Taylor expansion of $\Pi_G(l^2)$ yields:

$$\Pi_G(l^2) = \Pi_{Gu} - K_{Gu}(l^2 - l_u^2)/l_u^2 + \ldots \tag{11}$$

where $K_{Gu} = K_G(l_u^2)$ and $\Pi_{Gu} = \Pi_G(l_u^2)$. Equations (10) and (11) yield

$$\Delta F_l = \Pi_{Gu}(1 - l_x l_y/l_u^2) + \tfrac{1}{2} K_{Gu}(1 - l_x l_y/l_u^2)^2 + \ldots \tag{12}$$

During shear deformation, $l_l, l_l \to l_x, l_y$, assuming Gaussian chain statistics and using Eqs. (1) and (2), the change in gel elastic free energy per unit gel area of Ψ_u equals

$$\Delta F_s = \tfrac{1}{2} N_c k T (l_x - l_y)^2/(l_r l_u)^2 = \tfrac{1}{2} G (l_x/l_u - l_y/l_u)^2 . \tag{13}$$

The total change in elastic free energy associated with deforming the membrane gel, ΔF_{gel}, is then

given by

$$\Delta F_{\text{gel}} \equiv \int_{\Omega_{Gu}} \int (\Delta F_s + \Delta F_i)\, d^2r \approx \tfrac{1}{2} G\, I_1(\Omega_{Gu}) + \Pi_{Gu}\, I_2(\Omega_{Gu}) + \tfrac{1}{2} K_{Gu}\, I_3(\Omega_{Gu}), \tag{14}$$

where

$$I_1(\Omega_{Gu}) \equiv \int_{\Omega_{Gu}} \int (l_x/l_u - l_y/l_u)^2\, d^2r \tag{15}$$

$$I_2(\Omega_{Gu}) \equiv \int_{\Omega_{Gu}} \int (1 - l_x l_y/l_u^2)\, d^2r = -\Delta A_G \tag{16}$$

$$I_3(\Omega_{Gu}) \equiv \int_{\Omega_{Gu}} \int (1 - l_x l_y/l_u^2)^2\, d^2r\,. \tag{17}$$

The surface integration is done over the surface plane Ω_{Gu} of the membrane gel of Ψ_u; ΔA_G is the change in the membrane gel surface area when $\Psi_u \rightarrow \Psi_d$.

Cell shape dependent changes in the free energy of the membrane lipid bilayer

The change in membrane lipid bilayer elastic free energy because of changes in lipid monolayer surface areas resulting from cell shape change $\Psi_u \rightarrow \Psi_d$ equals

$$\Delta F_{\text{lipcom}} = -\int_{A_{Eu}}^{A_{Ed}} \Pi_E\, dA - \int_{A_{Pu}}^{A_{Pd}} \Pi_P\, dA\,, \tag{18}$$

where A is the lipid surface area and Π lipid surface tension. Subscripts u and d refer to cell shapes Ψ_u and Ψ_d. Subscripts E and P refer respectively to the extracellular and protoplasmic half of the membrane lipid bilayer.

Taylor expansion of Π_E and Π_P yields

$$\Pi_E(A) = \Pi_{Eu} - K_{Eu}(A - A_{Eu})/A_{Eu} \tag{19}$$

and analogously for $\Pi_P(A)$. Equations (18) and (19) yield

$$\Delta F_{\text{lipcom}} \approx -\Pi_{Eu}\Delta A_E - \Pi_{Pu}\Delta A_p + \tfrac{1}{2} K_{Eu}(\Delta A_E)^2/A_{Eu} + \tfrac{1}{2} K_{Pu}(\Delta A_P)^2/A_{Pu}\,, \tag{20}$$

where ΔA_E equals the difference between A_{Ed} and A_{Eu}, and ΔA_P equals the difference between A_{Pd} and A_{Pu}.

As a first approximation we have adopted Canham's (1970) expression for the bending energy of the two lipid monolayers:

$$\Delta F_{\text{lipben}} = \tfrac{1}{2} B_{Ed} \int_{\Omega_{Ed}} \int ((1/R_{E1} - 1/R_{E0})^2 + (1/R_{E2} - 1/R_{E0})^2)\, d^2r + \tfrac{1}{2} B_{Pd} \int_{\Omega_{Pd}} \int ((1/R_{P1} - 1/R_{P0})^2 + (1/R_{P2} - 1/R_{P0})^2)\, d^2r\,, \tag{21}$$

where B_{Ed} and B_{Pd} are the membrane lipid monolayer bending elastic moduli. R_{E1}, R_{E0}, R_{P1}, R_{P0} are the lipid monolayer principal radii of curvature. Ω_{Ed} and Ω_{Pd} are the surface of the lipid monolayers. The subscripts E and P refer respectively to the extracellular and protoplasmic half of the membrane lipid bilayer. When each membrane monolayer is assumed to behave like a homogeneous elastic material $B = K_M b^2/6$ where K_M is the modulus of area compression of the lipid monolayer and b is the thickness of the lipid monolayer (Canham 1970). Assuming $b = 2.5$ nm and using the values of K_M reported by Papahadjopoulos (1968) or deduced from the data of Lis et al. (1982), one calculates values for B_{Ed} and B_{Pd} in the range 10^{-13} to 10^{-12} dyne/cm. Evans (1983) reported that the erythrocyte membrane bending elastic modulus is approximately 1.8×10^{-12}dyne/cm, in good agreement with the estimates of the bending modulus of lipid bilayers presented here. Note that B_{Ed} and B_{Pd} are expected to depend strongly on lipid composition and environmental conditions (Papahadjopoulos 1968; Lis et al. 1982).

The elastic free energy master equation of the protein gel – lipid bilayer membrane model

The stable shape of a cell with no transcellular cytoskeleton is the shape which corresponds to the minimum value of the cell membrane total elastic free energy. Cell shapes which correspond to local minima in membrane free energy are metastable. If the energy barrier between metastable and stable is high in comparison to the thermal energy the spontaneous transformation rate from metastable to the stable cell shape may be very low.

The protein gel – lipid bilayer membrane model yields the following expression for the change in free energy for the cell shape change $\Psi_u \rightarrow \Psi_d$:

$$\begin{aligned}\Delta F_{\text{tot}} &= \Delta F_{\text{gel}} + \Delta F_{\text{lipcom}} + \Delta F_{\text{lipben}} \\ &\approx \tfrac{1}{2} G \int_{\Omega_{Gu}} \int (l_x/l_u - l_y/l_u)^2\, d^2r \\ &+ \tfrac{1}{2} K_{Gu} \int_{\Omega_{Gu}} \int (1 - l_x l_y/l_u^2)^2\, d^2r \\ &- (\Pi_{Gu}\Delta A_G + \Pi_{Eu}\Delta A_E + \Pi_{Pu}\Delta A_P) \\ &+ \tfrac{1}{2} K_{Eu}(\Delta A_E)^2/A_{Eu} + \tfrac{1}{2} K_{Pu}(\Delta A_P)^2/A_{Pu} \\ &+ \tfrac{1}{2} B_{Ed} \int_{\Omega_{Ed}} \int ((1/R_{E1} - 1/R_{E0})^2 + (1/R_{E2} - 1/R_{E0})^2\, d^2r \\ &+ \tfrac{1}{2} B_{Pd} \int_{\Omega_{Pd}} \int ((1/R_{P1} - 1/R_{P0})^2 + (1/R_{P2} - 1/R_{P0})^2)\, d^2r\,.\end{aligned} \tag{22}$$

Equation (22) is referred to as the elastic free energy master equation of the protein gel – lipid bilayer membrane model.

The magnitude of the error introduced in the master equation by ignoring the higher order terms in the Taylor expansion of Eqs. (10) and (18) depends on the non-linearity of gel osmotic tension versus gel area, the non-linearity of surface tension versus lipid area for each of the lipid bilayer halves, and the magnitudes of ΔA_G, ΔA_E, and ΔA_P.

Note that when $G \ll K_G$ the gel density will remain homogeneous when $\Psi_u \to \Psi_d$ and there will be a neutral plane with constant surface area located within the membrane and located the same distance from the gel for the entire cell surface. This distance will be determined by the geometric parameters a and b and the moduli of area compression K_E, K_P and K_G. For a pure lipid bilayer ($K_G = 0$) this neutral plane will be located within the lipid bilayer. For the erythrocyte membrane $G \ll K_E$ and $G \ll K_P$. This means that also for $G \sim K_G$ there will be a plane of unchanged surface area within the lipid bilayer when $\Psi_u \to \Psi_d$. However, because of the non-uniform gel density existing for such situations the coordinate z (Fig. 2) of this plane will no longer be the same over the entire cell surface.

At static equilibrium the sum of the tensions Π_{Gu}, Π_{Eu}, and Π_{Pu} is very close to zero. Increased negative value of Π_{Gu} therefore generally leads to increased positive values of Π_{Eu} and Π_{Pu}. By choosing the linear scaling factor between Ψ_r and Ψ_u such that

$$\Pi_{Gu} + \Pi_{Eu} + \Pi_{Pu} = 0 , \tag{23}$$

shape Ψ_u will be a metastable cell shape and the area changes ΔA_G, ΔA_E and ΔA_P resulting from $\Psi_u \to \Psi_d$ will for the reasons given above generally be small relative to A_G. Note that Eq. (23) does not assume that Π_G, Π_E, and Π_P vary linearly with ΔA_G, ΔA_E, and ΔA_P, respectively. Conrad and Singer (1979 and 1981) presented evidence for non-zero values of Π_{Eu} and Π_{Pu} in both erythrocyte and other cell membranes.

For any membrane plane located a short distance, z, from the gel plane, the change in surface area, ΔA, resulting from $\Psi_u \to \Psi_d$ can be expressed as

$$\Delta A \approx \Delta A_G + z\, \partial(\Delta A)/\partial z . \tag{24}$$

Note that the derivative $\partial(\Delta A)/\partial z$ depends only on the geometry of Ψ_u and Ψ_d, and not on the gel deformation of Ψ_d. Geometric considerations, and using Eqs. (23) and (24), the third term, T_3, of the master equation becomes

$$\begin{aligned} T_3 &\equiv -(\Pi_{Gu}\Delta A_G + \Pi_{Eu}\Delta A_E + \Pi_{Pu}\Delta A_P) \\ &= (\Pi_{Eu}(a + b/2) + \Pi_{Pu}(a + 3b/2))\, \partial(\Delta A)/\partial z , \end{aligned} \tag{25}$$

where the distances a and b are defined in Fig. 2. When $\Pi_{Gu} = 0$

$$T_3 = \Pi_{Pu}\, b\, \partial(\Delta A)/\partial z . \tag{26}$$

When $\Pi_{Gu} \neq 0$ term T_3 may be rewritten as

$$T_3 = -\Pi_{Gu}(a + b(\tfrac{1}{2} + (1 + \Pi_{Pu}/\Pi_{Eu})^{-1}))\, \partial(\Delta A)/\partial z \tag{27}$$

which is a particular useful expression when the effect of changing Π_{Gu} is studied for constant ratios Π_{Eu}/Π_{Pu}.

The bilayer couple hypothesis (Sheetz and Singer 1974) is the limiting case of the protein gel – lipid bilayer membrane model when $G \to 0$, $K_G \to 0$. The terms remaining are then the bilayer bending energy and the trilayer couple term which is now reduced to a bilayer couple term (Eq. (26)). In the accompanying paper (Stokke et al. 1986) we show that cell shapes with exocytotic protusions generally have negative $\partial(\Delta A)/\partial z$ whereas the opposite is the case for cell shapes with invaginations. For example, environmental conditions leading to a positive tension in the extracellular lipid monolayer therefore favour crenated cell shapes (Eq. (26)). The protein gel – lipid bilayer membrane model thus provides a firm molecular and theoretical basis for the concepts of the bilayer couple hypothesis. Even though the bilayer couple hypothesis incorporates an important mechanism for cell shape transformations, it will be shown that the bilayer couple hypothesis alone is completely unable to predict the observed stable shape within each erythrocyte shape class (Stokke et al. 1986). All the terms of the master equation generally have to be incorporated in the analysis to predict the stable and metastable cell shapes.

Membrane skeleton deformation for cell shape Ψ_d and contribution to cell shape stability

Here we will limit our analysis to the situation where both Ψ_u and Ψ_d have a global or local axis of rotational symmetry and the poles of the lipid bilayer and the membrane skeleton remain located adjacent to one another during the cell shape change $\Psi_u \to \Psi_d$ (Fig. 6). When both Ψ_u and Ψ_d have an axis of global rotational symmetry, a square gel area element of Ψ_u with edges of lengths l_u oriented parallel to, respectively, the local longitudinal and latitudinal line will deform into a rectangle on Ψ_d with edge lengths l_x and l_y. These edges will also be oriented parallel to the local longitudinal and latitudinal lines respectively, which means that the principal axes of the gel deformation point along the longitudinal and latitudinal lines of Ψ_u. For each gel

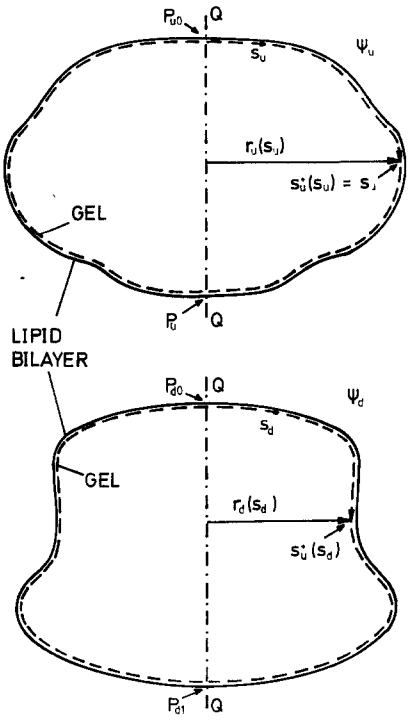

Fig. 6. Examples of cell shapes with global rotational symmetry. The axis of rotational symmetry passes through the membrane of cell shape Ψ_u at poles P_{u0} and P_{u1}, and of cell shape Ψ_d at poles P_{d0} and P_{d1}. s_u and s_d are the distances along the gel from pole P_{u0} for Ψ_u and from pole P_{d0} for Ψ_d, respectively, to the latitudinal line in question. The latitudinal line s_u^+ located a distance s_u from P_{u0} for Ψ_u will generally not be found at the same distance s_u^+ from P_{d0} for Ψ_d. The distance to the axis of rotational symmetry (Q–Q) of a gel latitudinal line located a distance s_u from P_{u0} for Ψ_u equals $r_u(s_u)$. When the latitudinal line is located a distance s_d from P_{d0} for Ψ_d the distance to Q–Q equals $r_d(s_d)$. The pole-to-pole distance along the gel surface for Ψ_u and Ψ_d equals P_u and P_d respectively

latitudinal line of Ψ_u we assign a parameter value s_u^+ being equal to the distance, s_u, along the gel from pole P_{u0} to the latitudinal line in question (Fig. 6). It is important to note that the parameter value s_u^+ is assigned to imagined physical lines along the gel, and that for Ψ_d the gel line s_u^+ will generally no longer be found at a distance $s_d = s_u$ from pole P_{d0}, that is $s_u^+ = s_u^+(s_d) \neq s_d$. The pole-to-pole distance along the gel surface of Ψ_u and Ψ_d we refer to as P_u and P_d respectively. When the gel is evenly stretched/compressed along the longitudinal lines, $s_u^+(s_d) = P_u s_d / P_d$ (Fig. 7). This we refer to as the "unrelaxed" state of the gel, but note that this state will generally not correspond to the minimum value of ΔF_{gel} for given Ψ_u and Ψ_d. When allowed to "relax", the gel will therefore spontaneously assume another density distribution (Fig. 7) which we refer to as the relaxed state of the gel. During gel relaxation the gel topology is assumed to remain unchanged.

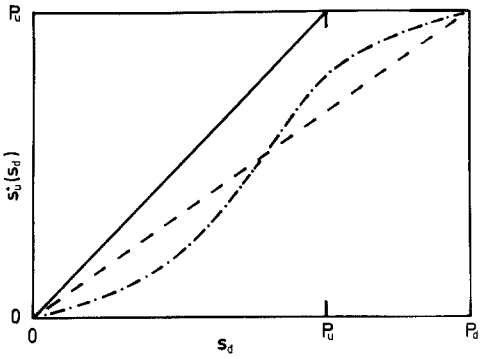

Fig. 7. Examples of gel latitudinal line s_u^+ versus the distance s_d from gel pole P_{d0} to the gel latitudinal line s_u^+. For Ψ_u the function $s_u^+(s_d)$ of the unrelaxed and relaxed gel is the same (——). Example of $s_u^+(s_d)$ for deformed cell shape, Ψ_d, with unrelaxed (– – –) and relaxed (– · – · –) gel

Geometric considerations yield

$$l_x / l_u = (r_d(s_d) / r_u(s_u^+(s_d))) \tag{28}$$

$$l_y / l_u = (ds_u^+(s_d)/ds_d)^{-1}, \tag{29}$$

where $r_d(s_d)$ is the distance from the axis of rotational symmetry to the latitudinal line located at a distance s_d along the surface from pole P_{d0} for Ψ_d (Fig. 6). Equations (15), (17), (28) and (29) yield

$$I_1(\Omega_{Gu}) = 2\pi \int_0^{P_d} [r_d(s_d)/r_u(s_u^+(s_d)) - (ds_u^+(s_d)/ds_d)^{-1}]^2 \cdot r_u(s_u^+(s_d))\,(ds_u^+(s_d)/ds_d)\,ds_d \tag{30}$$

$$I_3(\Omega_{Gu}) = 2\pi \int_0^{P_d} [1 - r_d(s_d)/r_u(s_u^+(s_d))/(ds_u^+(s_d)/ds_d)]^2 \cdot r_u(s_u^+(s_d))\,(ds_u^+(s_d)/ds_d)\,ds_d. \tag{31}$$

For known Ψ_u and Ψ_d, and thus $r_u(s_u)$, $r_d(s_d)$, P_u, and P_d, integrals I_1 and I_3 can be calculated when $s_u^+(s_d)$ is specified. The gel density distribution for given cell shapes Ψ_u and Ψ_d and the contribution, ΔF_1, to the membrane free energy due to the shear deformation and non-uniform gel compression can be determined by minimizing the calculated value of ΔF_1 with respect to the function $s_u^+(s_d)$.

For cell shapes with local rotational symmetry a certain fraction of the cell membrane maintains rotational symmetry. The poles P_{u0} and P_{d0} for each local membrane fraction, we define as for cells with global rotational symmetry. The boundary between the cell surface region with local rotational symmetry and the rest of the cell surface will be a latitudinal line of the region with local rotational symmetry. This boundary we refer to as pole line P_{u1} and P_{d1} for, respectively, the local cell shapes Ψ_u and Ψ_d. Analogous to the situation with global axial symmetry, we refer to the distance along the gel surface from pole P_{u0} to pole line P_{u1} as the pole-to-

pole distance P_u. P_d is defined analogously. Assuming that the same part of the gel is located within the region with local rotational symmetry for local cell shapes Ψ_u and Ψ_d and that Ψ_u and Ψ_d have the same surface area, the mathematical formulas derived for cells with global rotational symmetry is also valid for cells with local rotational symmetry.

In Appendix I it is shown that for constant G and cell shapes with global or local rotational symmetry the contribution from membrane skeleton shear deformation and non-uniform compression to the total free energy will decrease as K_{Gu} is reduced. As K_{Gu} is decreased, the favoured cell shape will therefore be determined to an increasing extent by the other terms in the free energy master equation. Since integrals I_1 and I_3 together always specify a unique favoured cell shape when $G \neq 0$ and $K_{Gu} \neq 0$ this means that as K_{Gu} is decreased there will at first normally be a decrease in cell shape stability accompanied by a some change in favoured cell shape until, finally, there may be a sharp shape transformation to an often completely different favoured cell shape. For example, the trilayer couple term predicts formation of exocytic or endocytic buds for large values of the gel osmotic tension, Π_{Gu}. A local change in the membrane skeleton environment leading to a local phase transition in the membrane skeleton and thereby a locally very small value of K_{Gu} may thus be a mechanism capable of initiating local exo- or endo-cytosis.

Human erythrocyte membrane skeleton shape Ψ_u

The stress-free shape of the membrane skeleton shape, Ψ_u, plays a central role in the mathematical theory of the protein gel – lipid bilayer membrane model. The two main features of Ψ_u are that the gel density is uniform and that there is no shear deformation in the gel. However, these criteria alone generally do not specify a unique shape Ψ_u for a given gel. For example, if a spherical cell shape satisfies these conditions, then all the other skeleton shapes shown in Fig. 8 also correspond to uniform gel density, no shear deformation and therefore the integrals I_1 and I_3 being equal to zero. Thus all of the shapes in Fig. 8 would be equally favoured by membrane skeleton shear deformation and non-uniform compression. It can further be shown that all the shapes Ψ_u depicted in Fig. 8 predict the same stable and metastable cell shapes and shape transformation. However, in the mathematical analysis it is normally most convenient to use the shape Ψ_u with no sharp edges. The equal energy shapes of the membrane skeleton (Fig. 8) provides an intuitive basis for the observed biconcave and cup-shaped cells as favoured cell shapes.

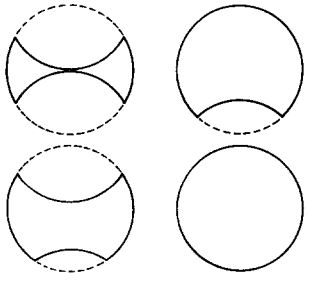

Fig. 8. Examples of skeletal shapes (——) which all correspond to zero gel shear deformation and zero non-local gel compression, when Ψ_u (---) is spherical

It is not known whether there exists a shape for which the erythrocyte membrane skeleton satisfies strictly the conditions of Ψ_u. But, because of the slow association equilibrium between the components of the spectrin network it is to be expected that if a certain cell shape, Ψ_d, is maintained unchanged for a long time (hours at 37 °C) the membrane skeleton will undergo stress relaxation and the cell shape Ψ_d will eventually satisfy the criterions for Ψ_u. If the cell shape, Ψ_d, is continuously changing, the unstrained gel shape, Ψ_u, will eventually equal the time average of Ψ_d. Rapid random deformations would lead to spherical Ψ_u.

Bull (1972) observed that the cavities and equator of biconcave erythrocytes can be relocated on the cell surface. This was taken to suggest that the mechanical properties of membranes are uniform over the entire cell surface which is the basis for the uniform shell hypothesis (Brailsford et al. 1976). For a macromolecular gel with perfectly uniform gel topology that makes up a closed surface, Ψ_u is spherical.

Lange et al. (1982) found that isolated spectrin shells often were disc-shaped. The presence of other components such as a certain amount of lipid in addition to spectrin in these shells complicates the interpretation, but Lange et al.'s observation suggests that the preparation procedure used by these authors yields erythrocyte membrane skeletons with discoid rather than spherical Ψ_u.

Concluding remarks

The concept that the membrane skeleton constitutes an ionic gel leads to predictions of the erythrocyte membrane elastic shear modulus and maximum elastic extension ratio which are close to the measured values. The recent discovery that ionic gels exhibit critical phenomena and can undergo phase transitions (Tanaka et al. 1980) introduces a theo-

retical basis for expecting that the erythrocyte membrane skeleton osmotic tension, Π_G, and the modulus of area compression, K_G, will be strongly dependent on environmental conditions. Our analysis shows that the magnitude of both Π_G and K_G can affect favoured cell shapes and cell shape stability. It will therefore be important to measure Π_G and K_G under a variety of environmental conditions.

The application of the protein gel – lipid bilayer membrane model may not be limited to the human erythrocyte membrane. Recent findings (Ben-Ze'ev et al. 1979; Tyler et al. 1980; Hartwig and Stossel 1981; Mescher et al. 1981; Luna et al. 1981; Bennett et al. 1982; Schliwa 1982; Nelson and Lazarides 1983; Glenney and Glenney 1983) show that long, flexible spectrin-like molecules are part of the membrane skeleton of many cells. No molecule by molecule information is required to derive the free energy master equation (Eq. (22)). The expression is valid for topologically replicating networks as well as randomly linked ones. This means that the predicted mechanochemical properties and the expression we have derived for the elastic free energy are valid also when the chain length and junction functionality vary randomly over the membrane skeleton. Our membrane model may therefore be used to predict important aspects of the mechanochemical properties and the elastic free energy of many different cell membranes containing a membrane skeleton.

Nucleated cells generally have a transcellular cytoskeleton apart from a possible membrane skeleton. The shape of such cells is the result of an interplay between the free energy of the membrane skeleton and the transcellular cytoskeleton. Although cytoskeleton structure may be dominated by the effects of dynamic events such as sliding and polymerization/depolymerization, considering the contributions of ionic gels to the mechanochemical properties of the membrane skeleton as well as the cytoskeleton may increase our general insight into the mechanisms of important aspects of cell shape transformations and cell motility.

Acknowledgement. We gratefully acknowledge the continued interest and encouragements of Dr. Daniel Branton throughout this study.

Glossary

a	distance from the middle of the gel to the lipid bilayer protoplasmic surface (Fig. 2)
b	thickness of each of the two cell membrane lipid bilayer halves (Fig. 2)
d	subscript denoting deformed cell shape Ψ_d
f_x	force needed in the x-direction to maintain the isotropic deformation $l_r, l_r \to l_x, l_y = l_x$
g	number of effective dissociated hydrogen ions per gel chain
k	the Boltzmann constant (1.38×10^{-38} Nm/K)
l_c	contour length of gel chain
$\langle l_{e-e} \rangle$	time average end-to-end distance of the gel chains in the reference state and thus the time average distance between topological first neighbour junctions in this state
l_l^2	area of the gel element with edge length l_x and l_y
$\langle l_{n-n} \rangle$	time average distance between nearest neighbour junctions of the gel
l_r	edge length of a square-shaped gel area element of Ψ_l which contains N_c gel chains. For Ψ_u this gel area element is a square with edge length l_u
l_s	segment length of chain molecule consisting of N_s identically freely jointed segments
l_u	edge length of a square-shaped gel area element of cell shape Ψ_u which contains N_c gel chains
l_x, l_y	edge lengths of a rectangular gel area element of Ψ_d which contains N_c gel chains, and for which Ψ_u is a square with edge length l_u
r	subscript denoting reference cell shape Ψ_r
r_u, r_d	distance from axis of global rotational symmetry to gel surface for cell shape Ψ_u and Ψ_d, respectively (Fig. 6)
s_l	$(i = u, d)$ distance from pole P_{i0} measured along the gel surface for cell shape Ψ_l (Fig. 6)
s_u^+	gel latitudinal line, which for Ψ_u is located a distance s_u from pole P_{u0}
u	subscript denoting undeformed cell shape Ψ_u
z	z-coordinate, perpendicular to and measured from the gel surface. Positive z-direction toward the interior of the cell (Fig. 2)
A_{ij}	$(i = E, P,\ j = u, d)$ surface area of the midplane of the lipid bilayer for the extracellular $(i = E)$ and protoplasmic $(i = P)$ half for cell shape Ψ_j
A_M	surface area of the macromolecules making up the rectangular gel area element with edge lengths l_u
B_{ij}	bending elastic modulus, subscripts as for A_{ij}
E	extracellular half of the cell membrane lipid bilayer (Fig. 2)
E	subscript denoting extracellular half of the cell membrane lipid bilayer
G	equilibrium elastic shear modulus
G	subscript denoting protein gel
$I_i(\Omega_{Gu})$	$(i = 1, 2$ and $3)$ integrals over the gel surface area Ω_{Gu} (Eqs. (15) and (17))
K_A	spectrin dimer-tetramer association constant
K_{Gj}	$(j = u, d)$ modulus of area compression of the protein gel for Ψ_j
K_{ij}	$(i = E, P,\ j = u, d)$ modulus of area compression for lipid monolayers. Subscripts as for A_{ij}
K_M	modulus of area compression for planar lipid monolayers
$L(\beta)$	Langevin function (Eq. (6))
N_A	Avogadro's number (6.024×10^{23} mole^{-1})
N_c	number of gel chains in the square gel area element with edge length l_u for Ψ_u
N_s	number of freely jointed identical segments each of length l_s in one gel chain
P	protoplasmic half of the cell membrane lipid bilayer (Fig. 2)
P	subscript denoting protoplasmic half of the cell membrane lipid bilayer
P_l	$(l = u, d)$ pole-to-pole distance measured along the surface for cell shape Ψ_l
P_{ij}	$(i = u, d,\ j = 0, 1)$ poles for cell shape Ψ_i
R_0	radius of the spherical gel

R_{0i} ($i = E, P$) radius of curvature of the unstrained lipid monolayer

R_{ij} ($i = 1, 2$ and $j = E, P$) principal radius of curvature

$[S]$ spectrin tetramer concentration when all spectrin is present as tetramers

T absolute temperature

T_3 third term of Eq. (22)

V_1 equivalent molar area of the gel solvent

ε, ε_{max} gel extension ratio and maximum extension ratio

ν_r number of chains per unit area for the gel reference state

φ', φ'_i two-dimensional protein gel area fraction for respectively an arbitrarily chosen state and the reference state

ΔA_i ($i = E, P, G$) change in midplane surface area when $\Psi_u \rightarrow \Psi_d$ for the membrane part indicated by the subscripts

ΔF_1 change in membrane free energy due to gel shear deformation and non-uniform gel compression when $\Psi_u \rightarrow \Psi_d$ (Eq. (A1))

ΔF_c free energy decrease associated with the formation of contact between protein gel chain segments

ΔF_{gel} change in total elastic free energy of the cell membrane protein gel when $\Psi_u \rightarrow \Psi_d$

$\Delta F_i, \Delta F_s$ elastic free energy per unit gel area of Ψ_u for respectively pure isotropic and pure shear deformation of the cell membrane protein gel area element for which Ψ_d is a square with edge length l_u

ΔF_{lipben} change in free energy because of lipid bending resulting from $\Psi_u \rightarrow \Psi_d$

ΔF_{lipcom} change in free energy because of lipid compression resulting from $\Psi_u \rightarrow \Psi_d$

ΔF_l elastic free energy associated with the rubber elasticity of the cell membrane protein gel assuming Gaussian chain statistics

ΔF_{tot} equals $\Delta F_{gel} + \Delta F_{lipcom} + \Delta F_{lipben}$

Π_{ij} ($i = E, P, G$, $j = u, r$) isotropic surface tension or osmotic surface tension for cell shape Ψ_j

Φ gel junction functionality

Ψ_d deformed cell shape with the same gel surface as Ψ_u

Ψ_r reference (neutral) cell shape, for which the time average gel chain configuration is the same as for the free chains, the gel density is uniform, and the gel shear deformation is zero over the entire cell surface

Ψ_s cell shape of the stable cell

Ψ_u cell shape obtained by linear scaling of Ψ_r

Ω_{Ed}, Ω_{Pd} midplane surface of respectively the extracellular and protoplasmic half of the lipid bilayer for Ψ_d

Ω_{Gu} protein gel surface for Ψ_u

References

Bennett V (1982) The molecular basis for membrane-cytoskeleton association in human erythrocytes. J Cell Biochem 18:49–65

Bennett V, Davis J, Fowler WE (1982) Brain spectrin, a membrane-associated protein related in structure and function to erythrocyte spectrin. Nature 299:126–131

Ben-Ze'ev A, Duerr A, Solomon F, Penman S (1979) The outer boundary of the cytoskeleton: a lamina derived from plasma membrane proteins. Cell 17:859–865

Brailsford JD, Korpman RA, Bull BS (1976) The red cell shape from discocyte to hypotonic spherocyte – A mathematical delineation based on a uniform shell hypothesis. J Theor Biol 60:131–145

Branton D, Cohen CM, Tyler J (1981) Interaction of cytoskeletal proteins on the human erythrocyte membrane. Cell 24:24–32

Bull B (1972) The red cell biconcavity and deformability. A macromodel based on flow chamber observations. Nouv Rev Fr Hematol 12:835–844

Byers T, Branton D (1985) Visualization of the protein associations in the erythrocyte membrane skeleton. Proc Natl Acad Sci USA 82:6153–6157

Canham PB (1970) The minimum energy of bending as a possible explanation of the biconcave shape of the human red blood cell. J Theor Biol 26:61–81

Cantor CR, Schimmel PR (1980) Biophysical chemistry, vol III. The behavior of biological macromolecules. WH Freeman, San Francisco

Chien S, Sung KLP, Skalak R, Usami S, Tøzeren A (1978) Theoretical and experimental studies on viscoelastic properties of erythrocyte membrane. Biophys J 24:463–487

Clarke M (1971) Isolation and characterization of a water-soluble protein from bovine erythrocyte membranes. Biochem Biophys Res Commun 45:1063–1070

Cohen CM (1983) The molecular organization of the red cell membrane skeleton. Sem Hematol 20:141–158

Cohen CM, Tyler JM, Branton D (1980) Spectrin-actin associations studied by electron microscopy of shadowed preparations. Cell 21:875–883

Conrad MJ, Singer SJ (1979) Evidence for a large internal pressure in biological membranes. Proc Natl Acad Sci USA 76:5202–5206

Conrad MJ, Singer SJ (1981) The solubility of amphipathic molecules in biological membranes and lipid bilayers and its implications for membrane structure. Biochemistry 20:808–818

Deuling HJ, Helfrich W (1976) Red blood cell shapes as explained on the basis of curvature elasticity. Biophys J 16:861–868

Dunbar JC, Ralston GB (1981) Hydrodynamic characterization of the heterodimer of spectrin. Biochim Biophys Acta 667:177–184

Elgsaeter A (1978) Human spectrin. I. A classical light scattering study. Biochim Biophys Acta 536:235–244

Elgsaeter A, Branton D (1974) Intramembrane particle aggregation in erythrocyte ghosts. I. The effects of protein removal. J Cell Biol 63:1018–1030

Elgsaeter A, Shotton DM, Branton D (1976) Intramembrane particle aggregation in erythrocyte ghosts. II. The influence of spectrin aggregation. Biochim Biophys Acta 426:101–122

Evans EA (1973) New membrane concept applied to the analysis of fluid shear- and micropipette-deformed red blood cells. Biophys J 13:941–954

Evans EA (1983) Bending elastic modulus of red blood cell membrane derived from buckling instability in micropipet aspiration tests. Biophys J 43:27–30

Evans E, Buxbaum K (1981) Affinity of red blood cell membrane for particle surfaces measured by extent of particle encapsulation. Biophys J 34:1–12

Evans EA, La Celle PL (1975) Intrinsic material properties of the erythrocyte membrane indicated by mechanical analysis of deformation. Blood 45:29–43

Evans EA, Skalak R (1979) Mechanics and thermodynamics of biomembranes, Parts 1 and 2. Crit Rev Bioeng 3:181–418

Flory PJ (1953) Principles of polymer chemistry. Cornell University Press, Ithaca, New York

Flory PJ (1976) Statistical thermodynamics of random networks. Proc R Soc London A 351:351–380

Flory PJ (1977) Theory of elasticity of polymer networks. The effect of local constraints on junctions. J Chem Phys 66: 5720–5729

Glenney JR Jr, Glenney P (1983) Fodrin is the general spectrin-like protein found in most cells whereas spectrin and the TW protein have a restricted distribution. Cell 34: 503–512

Goodman SR, Shiffer K (1983) The spectrin membrane skeleton of normal and abnormal erythrocytes: a review. Am J Physiol 244 (Cell Physiol 13): C121–C141

Gratzer WB (1983) The cytoskeleton of the red blood cell. In: Stracher A (ed) Muscle and nonmuscle motility. Academic Press, New York, pp 37–124

Gratzer WB (1984) More red than dead. Nature 310:368–369

Hartwig JH, Stossel TP (1981) Structure of macrophage actin-binding protein molecules in solution and interacting with actin filaments. J Mol Biol 145:563–581

Johnson RM, Robinson J (1976) Morphological changes in asymmetric erythrocyte membranes induced by electrolytes. Biochem Biophys Res Commun 70:925–931

Johnson RM, Taylor G, Meyer DB (1980) Shape and volume changes in erythrocyte ghosts and spectrin-actin networks. J Cell Biol 86:371–376

Kam Z, Josephs R, Eisenberg H, Gratzer WB (1977) Structural study of spectrin from human erythrocyte membranes. Biochemistry 16:5568–5572

Lange Y, Hadesman RA, Steck TL (1982) Role of the reticulum in the stability and shape of the isolated human erythrocyte membrane. J Cell Biol 92:714–721

Lemaigre-Dubreuil Y, Henry Y, Cassoly R (1980) Rotational dynamics of spectrin in solution and ankyrin bound in human erythrocyte membrane. FEBS Lett 113:231–234

Lemaigre-Dubreuil Y, Cassoly R (1983) A dynamical study on the interactions between the cytoskeleton components in the human erythrocyte as detected by saturation transfer electron paramagnetic resonance of spin-labeled spectrin, ankyrin, and protein 4.1. Arch Biochem Biophys 223: 495–502

Lis LJ, McAlister M, Fuller N, Rand RP, Parsegian VA (1982) Measurement of the lateral compressibility of several phospholipid bilayers. Biophys J 37:667–672

Liu SC, Palek J (1980) Spectrin tetramer-dimer equilibrium and the stability of erythrocyte membrane skeletons. Nature 285:586–588

Liu SC, Windisch P, Kim S, Palek J (1984) Oligomeric states of spectrin in normal erythrocyte membranes: Biochemical and electron microscopic studies. Cell 37:587–594

Luna EJ, Fowler VM, Swanson J, Branton D, Taylor DL (1981) A membrane cytoskeleton from *Dictyostelium discoideum*. I. Identification and partial characterization of an actin-binding activity. J Cell Biol 88:396–409

Mescher MF, Jose MJL, Balk SP (1981) Actin-containing matrix associated with the plasma membrane of murine tumour and lymphoid cells. Nature 289:139–144

Morrow JS, Marchesi VT (1981) Self-assembly of spectrin oligomers in vitro: A basis for a dynamic cystoskeleton. J Cell Biol 88:463–468

Mikkelsen A, Elgsaeter A (1978) Human spectrin. II. An electro-optic study. Biochim Biophys Acta 536:245–251

Mikkelsen A, Elgsaeter A (1981) Human spectrin. V. A comparative electro-optic study of heterotetramers and heterodimers. Biochim Biophys Acta 668:74–80

Mikkelsen A, Stokke BT, Elgsaeter A (1984) An electro-optic study of human erythrocyte spectrin dimers. The presence of calcium ions does not alter spectrin flexibility. Biochim Biophys Acta 786:95–102

Nelson WJ, Lazarides E (1983) Expression of the β subunit of spectrin in nonerythroid cells. Proc Natl Acad Sci USA 80:363–367

Nicolson GL, Marchesi VT, Singer SJ (1971) The localization of spectrin on the inner surface of human red blood cell membranes by ferritin-conjugated antibodies. J Cell Biol 51:265–272

Papahadjopoulos D (1968) Surface properties of acidic phospholipids: Interaction of monolayers and hydrated liquid crystals with uni- and bivalent metal ions. Biochim Biophys Acta 163:240–254

Pinto da Silva P (1972) Translational mobility of the membrane intercalated particles of human erythrocyte ghosts. pH-dependent, reversible aggregation. J Cell Biol 53: 777–787

Ralston GB (1976) Physico-chemical characterization of the spectrin tetramer from bovine erythrocyte membranes. Biochim Biophys Acta 455:163–172

Reich MH, Kam Z, Eisenberg H, Worcester D, Ungewickell E, Gratzer WB (1982) Solution scattering studies of dimeric and tetrameric spectrin. Biophys Chem 16:307–316

Scanus E, Booth S, Hallaway B, Rosenberg A (1985) The elasticity of spectrin-actin gels at high protein concentration. J Biol Chem 260:3724–3730

Schliwa M (1982) Action of cytochalasin D on cytoskeletal networks. J Cell Biol 92:79–91

Sheetz MP, Singer SJ (1974) Biological membranes as bilayer couples. A molecular mechanism of drug-erythrocyte interactions. Proc Natl Acad Sci USA 71:4457–4461

Shotton DM, Burke BE, Branton D (1979) The molecular structure of human erythrocyte spectrin. Biophysical and electron microscopic studies. J Mol Biol 131:303–329

Siegel DL, Branton D (1985) Partial purification and characterization of an actin-bundling protein, band 4.9, from human erythrocytes. J Cell Biol 100:775–785

Skalak R, Tozeren A, Zarda RP, Chien S (1973) Strain energy function of red blood cell membranes. Biophys J 13: 245–264

Speicher DW, Marchesi VT (1984) Erythrocyte spectrin is comprised of many homologues triple helical segments. Nature 311:177–180

Steck TL (1974) The organization of proteins in the human red blood cell membrane. J Cell Biol 62:1–19

Stokke BT, Elgsaeter A (1981) Human spectrin. VI. A viscometric study. Biochim Biophys Acta 640:640–645

Stokke BT, Mikkelsen A, Elgsaeter A (1985a) Human erythrocyte spectrin dimer intrinsic viscosity: Temperature dependence and implications for the molecular basis of the erythrocyte membrane free energy. Biochim Biophys Acta 816:102–110

Stokke BT, Mikkelsen A, Elgsaeter A (1985b) Some viscoelastic properties of human erythrocyte spectrin end-linked in vitro. Biochim Biophys Acta 816:111–120

Stokke BT, Mikkelsen A, Elgsaeter A (1986) The human erythrocyte membrane skeleton may be an ionic gel. II. Numerical analyses of cell shapes and shape transformations. Eur Biophys J 13:219–233

Tanaka T, Fillmore D, Sun ST, Nishio I, Swislow G, Shah A (1980) Phase transitions in ionic gels. Phys Rev Lett 45: 1636–1639

ter Haar D, Wergeland H (1966) Elements of thermodynamics. Addison-Wesley, London

Treloar LRG (1975) The physics of rubber elasticity. 3rd edit. Clarendon Press, Oxford

Tyler JM, Anderson JM, Branton D (1980) Structural comparison of several actin-binding macromolecules. J Cell Biol 85:489–495

Ungewickell E, Gratzer W (1978) Self-association of human spectrin. A thermodynamic and kinetic study. Eur J Biochem 88:379–385

Waugh R, Evans EA (1979) Thermoelasticity of red blood cell membrane. Biophys J 26:115–132

Appendix I

The membrane skeleton contribution to the shape stability of cell shapes with rotational symmetry

For given Ψ_u, environmental conditions and possible restraints on Ψ_d the stable cell shape, Ψ_s, is the cell shape Ψ_d associated with the lowest value of ΔF_{tot}. The stability of cell shape Ψ_s is determined by the increase in ΔF_{tot} associated with changing the cell shape from Ψ_s to another resembling cell shape Ψ_d. The cell will give the overall impression of being rigid if this increase is large, and soft if the increase is small. The contribution, ΔF_1, to the membrane free energy due to the shear deformation and non-uniform spectrin gel compression equals

$$\Delta F_1 = \tfrac{1}{2} G I_1 + \tfrac{1}{2} K_{Gu} I_3 . \tag{A1}$$

In the case of a phase separation situation in the spectrin gel where K_{Gu} ideally equals zero, Eq. (30) yields that $I_1 = 0$ for any cell shape Ψ_d if

$$ds_u^+(s_d)/ds_d = r_u(s_u^+(s_d))/r_d(s_d) \tag{A2}$$

for all $0 < s_d < P_d$. The boundary conditions for the function $s_u^+(s_d)$ which yields $I_1 = 0$ are

$$s_u^+(s_d = 0) = 0 \tag{A3}$$

$$s_u^+(s_d = P_d) = P_u . \tag{A4}$$

To correspond to possible physical solutions $r_u(s_u)$ and $r_d(s_d)$ must be continuous and for cell shapes with global axial symmetry satisfy the conditions

$$r_u(s_u = 0) = r_u(s_u = P_u) = r_d(s_d = 0) = r_d(s_d = P_d) = 0 . \tag{A5}$$

It is very important to note that although Eq. (A2) is a first-order differential equation in $s_u^+(s_d)$ the two boundary conditions for $s_u^+(s_d)$ given by Eqs. (A3) and (A4) do not make the system overdetermined. In fact, because of the restrictions on r_u and r_d given by Eq. (A5), rendering $ds_u^+(s_d)/ds_d$ undetermined both for $s_d = 0$ and $s_d = P_d$, one condition in addition to those given by Eqs. (A3) and (A4) has to be provided in order to specify a unique solution $s_u^+(s_d)$ satisfying Eqs. (A2), (A3) and (A4).

When $r_d(s_u) = r_u(s_u)$ (that is, Ψ_u equals Ψ_d) the function $s_u^+(s_d) = s_u$ will automatically satisfy Eq. (A2) and the boundary conditions, and therefore $I_1 = 0$. Since the integrand of I_1 always is positive, this is the minimum value of I_1. However, it is important to note that there will be a continuum of other functions $s_u^+(s_d)$ that satisfy Eq. (A2) and the boundary conditions Eqs. (A3) and (A4) when $r_d(s_u) = r_u(s_u)$. These functions can for example be obtained numerically using the following difference form of Eq. (A2):

$$s_{u,n+1}^+ = s_{u,n} + (r_u(s_{u,n}^+)/r_d(n P_d/N))\,(P_d/N) , \tag{A6}$$

where

$$s_{u,n}^+ \equiv s_u^+(s_d = n P_d/N) \quad 0 < n < N-1 . \tag{A7}$$

Parameter N is the number of equal intervals into which P_d has been divided. Figure 9A shows $s_u^+(s_d)$ when $r_u(s_u) = r_d(s_u) = R_0 \sin(\pi s_u/P_u)$, where R_0 is the radius of the spherical gel. Figure 9B shows $s_u^+(s_d)$ when $r_d(s_d)$ corresponds to a flat disc with surface area equal $4\pi R_0^2$ and $r_u(s_u) = R_0 \sin(\pi s_u/P_u)$. Note that also when $r_u(s_u) \neq r_d(s_d)$ there will generally be a continuum of functions $s_u^+(s_d)$ which satisfies Eq. (A2) and the boundary conditions Eqs. (A3) and (A4), as long as $r_u(s_u)$ and $r_d(s_d)$ satisfy Eq. (A5). This means (Eq. (A1)) that for $K_{Gu} = 0$ a continuum of cell shapes Ψ_d is energetically equally favourable by a gel strictly following Gaussian chain statistics. In addition there will for every favoured Ψ_d be a continuum of different gel density distributions characterized by $s_u^+(s_d)$ which all also are energetically equally favourable.

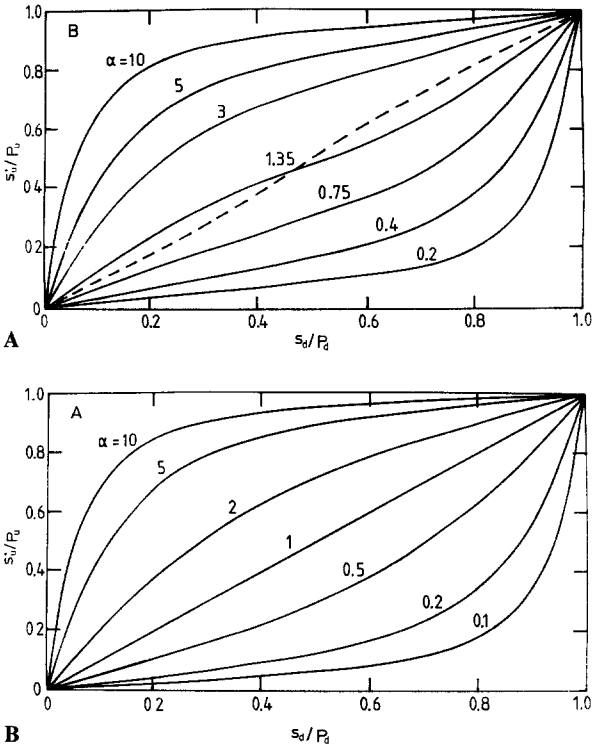

Fig. 9. Examples of functions $s_u^+(s_d)$ which yield $I_1 = 0$ for spherical Ψ_u with radius R_0 ($r_u(s_u) = R_0 \sin(\pi s_u/P_u)$) and (**A**) spherical Ψ_d with radius R_0 ($r_d(s_u) = r_u(s_u)$) or (**B**) Ψ_d being a flat disc with total surface area $A = 4\pi R_0^2$ ($r_d(s_d) = s_d$ for $0 < s_d < R_0\sqrt{2}$ and $r_d(s_d) = R_0 2\sqrt{2} - s_d$ for $R_0\sqrt{2} < s_d < R_0 2\sqrt{2}$). The gel density distribution corresponding to $s_u^+(s_d)$ which yields $I_3 = 0$ for example (B) is also shown (– – – –). The numerical solutions were obtained using Eq. (A6), $s_{u,0}^+ = 0$, and $s_{u,1}^+ = \alpha P_d/N$, where α is a variable parameter and $N = 100$

Equation (31) yields $I_3 = 0$ when

$$r_u(s_u^+)\, ds_u^+ = r_d(s_d)\, ds_d \tag{A8}$$

for all $0 < s_d < P_d$. Since $s_u^+(s_d = 0) = 0$, Eq. (A8) yields

$$\int_0^{s_u^+} r_u(x)\, dx = \int_0^{s_d} r_d(x)\, dx\,. \tag{A9}$$

For given $r_u(s_d)$ and $r_d(s_d)$ there will therefore always be one function $s_u^+(s_d)$ given by Eq. (A9) which yields $I_3 = 0$. The function $s_u^+(s_d)$ which yields $I_3 = 0$ for Ψ_u being spherical and Ψ_d being a flat disc is shown in Fig. 9B. This means (Eq. (A1)) that also for $G = 0$ a continuum of cell shapes Ψ_d is energetically equally favourable when the gel strictly follows Gaussian chain statistics. However, since the same function $s_u^+(s_d)$ generally does not yield both $I_1 = 0$ and $I_3 = 0$ (Fig. 9B), the free energy ΔF_1 will normally have minimum for one particular Ψ_d and $s_u^+(s_d)$ when neither G nor K_{Gu} are equal to zero.

For local cell shape rotational symmetry $ds_u^+(s_d)/ds_d$ is not undetermined for $s_d = P_d$ and there will therefore only be one function $s_u^+(s_d)$ and not a continuum of functions which yields $I_1 = 0$ as is the case for global cell shape rotational symmetry. Except for this difference, the stability features are the same for cell shapes with local and global rotational symmetry.